Journal of the Optical Society of America B
OPTICAL PHYSICS

Thermal nonlinear optical responses of native and oxidized low-density lipoprotein solutions at visible and infra-red wavelengths: complementary approaches

F. L. S. Cuppo,* A. R. N. Santisteban, and A. M. Figueiredo Neto

Department of Experimental Physics, Institute of Physics, University of São Paulo, São Paulo, SP, Brazil
**fcuppo@alumni.usp.br*

Received 29 November 2023; revised 23 May 2024; accepted 24 May 2024; posted 24 May 2024; published 12 June 2024

Single beam *Z*-scan (ZS) experiments at 532 nm (visible) and 979 nm [infra-red (IR)] wavelengths were used to determine photothermal responses of native and oxidized aqueous suspensions of human low-density lipoproteins (LDLs). The wavelengths employed in the measurements were chosen according to the optical absorption solute (LDL particles) and solvent (water) of the suspension. At 532 nm, water presents negligible absorbance, and the LDL is responsible for the light absorption. On the other hand, at 979 nm, the water is the main light absorber. In the visible light case, the particles absorb the laser light and, by conduction, transfer heat to water to form the thermal lens. In the IR experiments, water is the main absorber and transfers the heat to the particles to form the thermal lens. We show that with the IR light it is possible to investigate high degrees of oxidation of LDL, not possible with the usual visible light experiments. Differently from the usual ZS experiments with LDL at visible light, the magnitude of the thermal lens formed in the IR experiments was shown to be bigger in oxidized samples with respect to that of the native samples. For both wavelengths, all samples whose response was measured presented negative nonlinearity (self-defocusing behavior). It was also observed, in experiments with IR light, that the formation time of the thermal lens tends to decrease with the increase in the degree of oxidation of the sample.

https://doi.org/10.1364/JOSAB.514786

1. INTRODUCTION

The *Z*-scan (ZS) technique is a very efficient way for determining the third order nonlinear response from different origins, based on the exposure time of samples to a focused laser beam [1]. In a summarized way, for the closed aperture (transmittance measurement) configuration, the ZS setup employs a lens that focuses a polarized Gaussian intensity profile beam into a narrow waist along the z direction (propagating axis). An iris, placed in the far field, centered in the z-axis, is used to measure the light transmittance across the sample. The sample is moved through the focal point in steps and the transmitted light is measured as a function of the z position of the sample. A physical model was developed to describe nonlinearities from electronic origin. By carrying out small developments with respect to the original proposed experimental setup and/or data acquisition, a ZS measurement can provide information on nonlinearity effects from different origins [2]. A time-resolved data acquisition method was proposed to describe the time-evolution effect of slow absorbers [3]. This method is also used in data analysis of ZS results originated from thermal effects. Originally, the ZS technique was proposed for a local response effect, and the thermal effect is nonlocal in space and time, but, under some circumstances, it is possible to find an equivalence between the phase distortion generated by a thermal lens [4], and the original theory [5]. A further development of the thermal-lens model was proposed to account for the thermodiffusion phenomenon, employing a ZS experiment, just conveniently choosing the time scale of the laser pulse [6].

The thermal-origin response of aqueous systems is measured when a sample is exposed to the beam with durations from a few milliseconds to seconds and there are results reported for a wide range of aqueous media such as lyotropic liquid crystals [7], lyotropic-like aggregates [8], ferrofluids [9], and several biological materials like proteins [10], cholesterol/triglycerides [11], blood glucose [12], creatinine [13], etc.

Despite the fact that the ZS technique has been used to investigate solutions where the solute is the main absorber of the energy from the laser beam, to the best of our knowledge, the formation of the thermal lens due to the light absorption by the solvent, and the obtaining of complementary information about the solute with this procedure, have not been reported in the literature. In this context, our paper discusses the advantages

of using different light wavelengths to explore the properties of a particular solute in a solution. This aspect is particularly important if the solute, being the main absorber, may change its properties due to the light absorbance.

Among biological materials, lipoproteins have aroused the interest of several studies due to their relationship with health-related topics such as cardiovascular disease [14,15]. Lipoproteins are complex particles that have a hydrophobic core surrounded by a hydrophilic shell. The core is composed of non-polar lipids, cholesterol esters, and triglycerides, while the shell is made of phospholipids, free cholesterol, and apolipoproteins [16,17]. The ZS technique, in millisecond exposition-time configuration, using visible light to excite the sample (532 nm), has been used to characterize the lipoprotein's response to *in vitro* and *in vivo* modifications (mainly oxidation) [18,19]. There are interesting issues related to changes in the optical response of lipoproteins subjected to oxidation [20]. In the case of the low-density lipoprotein (LDL), oxidation products, as phospholipid hydroperoxides and cholesterol ester hydroperoxides, are formed in the process. The main absorbers (at 532 nm) of native (non-oxidized) LDL particles are the carotenoids [21,22]. During oxidation (or modification), *in vitro* or *in vivo*, the number of carotenoids in the particles decreases, since this group of pigment molecules (yellow to red color) is part of the first protection barrier of the LDLs against oxidation [23–27].

In this framework, the solute is responsible for the formation of the thermal lens in the solution, heating the solvent (water) by conduction. The amplitude of the thermal lens was shown to decrease with the sample oxidation [15,19]. It is known that there are multiple ways in which carotenoids can be modified, including auto-oxidation, free radicals present in the medium, thermal degradation, and light exposition processes, such as photodegradation and photo-isomerization [28,29].

The effect of illuminating carotenoids with a wavelength of 532 nm is expected to be much smaller than when exposed to radiation in the range 420–500 nm (where the absorption peaks are—for β-carotene—present in LDL: 428 nm, 456 nm, 482 nm [30]), but the effect is still present [22,30,31]. Carotenoids have as a chromophore a long conjugated double bond system that absorbs light strongly and exhibits intense main observation bands in the visible range (420–500 nm) and in some cases in the UV region, which allows their identification and characterization by methods such as UV-Vis spectroscopy, allowing them to shine with other optical or separation methods [32,33]. So, the use of the 532 nm light to investigate the properties of the LDL solution must be taken with care once this light may induce small modifications in the carotenoids and gives incomplete information about the LDL particles. Nevertheless, ZS has been shown to be a sensitive technique to LDL oxidation [18,19,27]. To minimize, or even avoid this problem in the *in vitro* experiments, chelating agent *ethylenediamine tetraacetic acid* (EDTA) is usually added to stop the oxidation of the LDL [34–36].

ZS simplicity makes it an interesting technique to be used in studies of LDL samples (oxidized or not) when compared to other available oxidized LDL (oxLDL) determination techniques such as spectrophotometry, colorimetry, fluorescence [37,38], etc. An alternative (and complementary procedure) to avoid the interaction of the carotenoids with the visible light is to heat the solution through the solvent, i.e., water. To achieve this task, we propose to employ a laser beam with wavelength of 979 nm in the ZS setup. At this wavelength the absorbance of the LDL native particles is negligible and that of water is much bigger. In this paper we compare the use of both wavelengths (532 and 979 nm) to show the characteristics of the thermal lenses formed in the LDL water-based solutions and the information got from the lipoprotein itself. For the 979 nm wavelength, water exhibits a significantly higher optical absorption coefficient with respect to that of visible wavelengths, three orders of magnitude higher: 4.74×10^{-1} cm^{-1} for 979 nm and 6.27×10^{-4} cm^{-1} for 532 nm [17].

2. THEORETICAL BACKGROUND

The thermal-lens model was first described analyzing the changing in the transmittance of a non-focused Gaussian beam [39], then expanded to a focused Gaussian beam [40,41]. In weakly absorbing media, a thermal lens is generated by a refraction-index gradient due to a rising in the local heating in the sample. Thermal-lens phenomena usually take place on a millisecond time scale [6]. There are two main models to analyze the thermal effect from data obtained in a ZS experiment: parabolic lens model and aberrant model [42,43]. These models have already been tested [4], and, in this paper, such as in others that investigate the thermal response of the lipoprotein solutions [18,19,35,36,44,45], due to its simplicity and convenience to be applied in a ZS experiment [5], the parabolic lens model is chosen.

The thermal-lens characteristic time formation, t_c, is position dependent and described by [4]

$$t_c = \frac{w(z)^2}{4}\frac{\rho C_p}{\kappa} = \frac{w(z)^2}{4D}, \tag{1}$$

where $w(z)$ is the beam waist at a position z, κ is the thermal conductivity, ρ and C_p are the volumetric density and the specific heat capacity, and $D = \rho C_p/\kappa$ is the thermal diffusivity. The beam waist can be written in terms of the beam waist at the focus, w_0, as [46]

$$w\,(z) = w_0\sqrt{\left[1+\left(\frac{z}{z_0}\right)^2\right]}, \tag{2}$$

and the parameter t_c can be rewritten, in terms of w_0, as

$$t_c = \frac{w_0^2\left[1+\left(\frac{z}{z_0}\right)^2\right]}{4D} = t_{cw_0}\left[1+\left(\frac{z}{z_0}\right)^2\right], \tag{3}$$

where z_0 is the Rayleigh length of the focused beam, which is related to the value of w_0 by $z_0 = \frac{\pi}{\lambda}w_0^2$ [46].

The magnitude of the phase distortion (θ) generated by the thermal lens is given by [4]

$$\theta = P\frac{\alpha L}{\lambda\kappa}\left(-\frac{dn}{dT}\right), \tag{4}$$

where α is the optical absorption, P is the beam power, L is the sample thickness, $\frac{dn}{dT}$ is the thermo-optic coefficient, and λ is the laser wavelength.

Since the thermal-lens formation process is a dynamic process, it is reasonable to think that the signal measured at the detector positioned in the far field will vary during lens formation. Furthermore, according to Eq. (1), each position in the scan has a characteristic lens formation time.

To present ZS results, it is convenient to work with a normalized position $x = (\frac{z}{z_0})$. Using the normalized position, normalized transmittance, in function of θ, t_{cw_0}, can be written as [4,5]

$$T_N(x, t) = \frac{1}{1 + \left\{\left[\frac{\theta}{(1+x^2)\frac{t_{cw_0}}{2t}}\right]\frac{2x}{(1+x^2)}\right\} + \left\{\left[\frac{\theta}{(1+x^2)\frac{t_{cw_0}}{2t}}\right]^2\frac{1}{(1+x^2)}\right\}}. \quad (5)$$

The normalized transmittance curve presents a peak and a valley, and the value of the difference between these two values (ΔT_{PV}), in the thermal-lens model, when the lens formation process is close to saturation (i.e., $t \gg t_{cw_0}$), is related to phase distortion θ by $\Delta T_{PV} \approx 2\theta$. The z-axis separation between the peak and valley (Δz_{PV}), for the parabolic thermal-lens model, is $\Delta z_{PV} \approx 2z_0$ [4]. Supplement 1 provides a basic presentation of the parabolic thermal-lens model that helps in understanding the normalized transmittance equation. In the document, Fig. S1 shows simulated ZS curves using Eq. (5) for fixed values of magnitude of the phase distortion and characteristic time of formation of the thermal lens at focus, and different beam exposure times. In this figure there is a clear increase in the observed effect (ΔT_{PV} value) with exposure time as well as the tendency towards saturation of the thermal effect.

3. SAMPLES AND EXPERIMENTAL SETUP

A. Separation of Low-Density Lipoproteins

Human plasma provided by "COLSAN - Associação Beneficiente de Coleta de Sangue, São Paulo, Brazil" was used to obtain LDL samples, by two-step serial ultracentrifugation [47,48]. The process is fully described in Supplement 1.

B. UV-Visible Spectroscopy

Optical absorption characterization, using light transmittance experiments, was employed to determine the relationship between the sample concentration and the absorbance of the LDL samples. The system used was composed by a DH-2000-BAL light source (deuterium and halogen-tungsten lamps—both operate simultaneously), Mikropack, providing radiation in the range 210–2500 nm (nominal), a USB4000 fiber optic spectrometer, Ocean Optics (currently Ocean Insight), which operates in the UV-VIS-NIR range: 200–1100 nm, and a temperature-controlled support at 37°C where the samples were positioned in. Light was sent to the sample by a system of multimodal optical fibers. Samples (140 µL) were placed in quartz cuvettes with 1 cm optical path for each measurement. In analyzing the extinction spectra, Rayleigh scattering was removed to obtain the sample's absorption. The experiment focused on the peak absorbance of carotenoids, which was measured at $\lambda = 484$ nm (characteristic wavelength absorption of carotenoid that is consumed during the oxidation process) [18]. Other absorption peaks were also observed between $\lambda = 200-300$ nm, which corresponded to other molecules present in LDL, such as ApoB-100, cholesterol, α-tocopherol, and phospholipids [49,50].

C. In vitro LDL Oxidation Essays

Samples of lipoproteins and control buffer solutions [potassium bromide (KBr) and potassium bromide solution with the addition of 30 µM of copper sulfate ($CuSO_4$); see Supplement 1] were used for UV-Vis and ZS measurements at five incubation times (0 h, 3 h, 4 h, 5 h, 6 h). To stop the oxidation, 0.05 mM of EDTA was added to the sample, after finishing the incubation period. The oxidation process requires time to cause appreciable changes in the optical response of LDL samples [18]; therefore, for short incubation times, less than 3 h, samples were not prepared as the thermal responses were shown to be not significant. Samples had labels according to the incubation period T0, T1, T2, T3, and T4, where T0 indicates 5 min ("fresh" sample); T1 indicates 3 h between sample preparation and measurement; T2 indicates 4 h; T3 indicates 5 h, and T4 indicates 6 h. For comparison purposes, sample buffer measurements were also performed with the same incubation times. Since the native and oxidized samples have EDTA, we do not expect a noticeable effect of the light (at 532 nm) to oxidize carotenoids during the ZS experiments.

D. *Z*-Scan Setups

The determination of nonlinear response from thermal origin was obtained with closed aperture ZS experiments in two independent time-resolved [3] setups, one with visible light and the other with infra-red (IR) light. Sketches of the experimental setups used are presented in Fig. S2 in Supplement 1. For the setup with visible light, a Verdi 2 CW laser, Coherent, was used, with a nominal wavelength of 532 nm, Gaussian intensity profile (TEM_{00}, $M^2 = 1.0$), maximum output power of 2 W, and exposure time adjusted with a chopper. In this setup we employed a 15 cm focal distance lens, beam waist at focus $w_0 = 28.4 \pm 0.7$ µm, and Rayleigh length of 4.78 ± 0.23 mm. For the IR setup, an OBIS 980 CW laser, Coherent, was used, with a nominal wavelength of 979 nm, Gaussian intensity profile (TEM_{00}, $M^2 = 1.1$), and maximum output power of 150 mW whose exposure was adjusted with a shutter. In this setup we employed a lens with 8.89 cm focal distance providing a beam waist at focus $w_0 = 55 \pm 3$ µm, with a Rayleigh length of 9.7 ± 1.2 mm. The beam waist values in both setups were determined using the knife-edge technique [51]. The values of z_0 were obtained directly from $z_0 = \frac{\pi}{\lambda}w_0^2$ [46].

Sample holders were made with two 1 mm thick rectangular glass plates (typically 15 × 8 mm) separated by a 200 µm Teflon spacer. The spacer-separated glasses were glued with inert epoxy resin. In the ZS measurements, 200 µm effective-thickness samples can be considered thin (much smaller than

z_0) for both experimental setups. For visible ZS measurements, lipoprotein samples were exposed to a 100 mW square wave beam for 30 ms—chopped beam configuration usually reported [44,52]—while for the 979 nm measurements, the same lipoprotein samples were exposed to a 95 mW light beam lasting 30 ms. Due to the greater optical absorption of water at this wavelength, a longer resting time was chosen (without the laser illumination), 470 ms, to ensure that the exposure process always took place with the sample at the same initial temperature. To have such different exposure and rest times, the laser beam was modulated using a shutter. The measurements were made with time resolution of 0.1 ms enabling a good determination of the temporal response of the thermal-lens formation in both setups. Empty sample holders showed no detectable nonlinear response at the measurement conditions for both setups.

The ZS curves presented are the result of the average of 10 independent runs for the visible light and five independent runs for the IR. All measurements were performed at 37°C.

4. RESULTS

Lipoproteins are described as native (Nat, no oxidation process, i.e., without addition of $CuSO_4$ solution, just left at rest) and oxidized (Ox, where there is an oxidation process during incubation time). Figure 1(a) shows the absorbance spectra of water and LDL samples in the wavelength ranges in which ZS experiments were performed. Lines with open geometric shapes represent native samples, and lines with filled geometric shapes represent oxidized samples. In the same figure, the dashed lines represent laser wavelengths 532 nm and 979 nm, and the dashed-dotted line represents the carotenoid absorption peak: 484 nm. In the range 450–570 nm it is possible to verify that the absorbance of LDL samples is greater for wavelengths shorter than 550 nm. Furthermore, a decrease in the absorbance values of samples that present oxidation is evident, mainly in the range 450–500 nm, due to carotenoids degradation [28,29]. It is also possible to observe that the absorption is larger for LDLnat samples (and T0 of LDLox) that were not exposed to the oxidation process. Water as well as buffers do not present considerable optical absorption in this range of wavelengths. For the range of infra-red wavelengths, all samples present absorbance with similar behavior, being numerically lower than the absorbance determined for pure water. In Fig. 1(b) the absorbance values of the samples are presented for the wavelengths used in the experiments. It is straightforward to note that for visible wavelengths the oxidation process reduces the measured absorbance (especially above 3 h of oxidation), while for IR wavelengths the curves are similar for all samples although oxidized samples present slightly lower values than native samples.

Pure water and buffers for native (KBr + EDTA) and oxidized (KBr + $CuSO_4$ + EDTA) sample absorbances in the visible range are negligible while, for 979 nm, pure water and buffers present absorbance values very similar to each other and larger than those of LDL samples investigated, and this happens since LDL components present in the sample have smaller optical absorption than that of water at this wavelength. It is possible to note that for 979 nm the absorbance values for the oxidized samples are slightly lower than for the native sample without a tendency for the difference in values to increase with increasing oxidation (trend observed for the wavelength of 532 nm).

A. *Z*-Scan at 979 nm

Figure 2 presents the ZS curves for water, lipoprotein samples (Nat and Ox, T0), and for lipoprotein samples with 6 h incubation time (Nat and Ox, T4). All the measurements

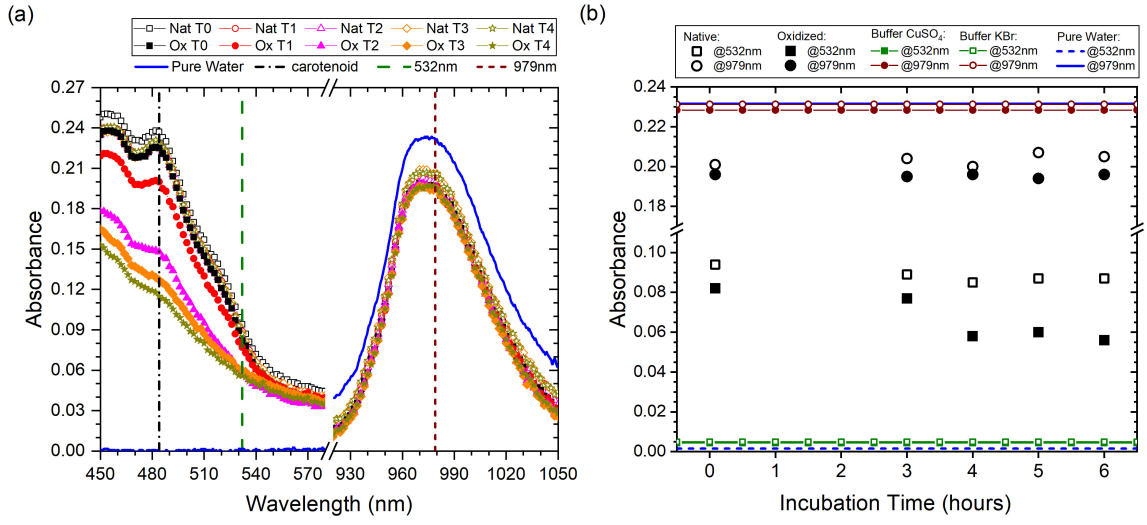

Fig. 1. (a) LDL absorbance as a function of the wavelength. Solid line is from water, native samples (no oxidation) are represented by lines with open geometric shapes, and oxidized samples are represented by lines with filled geometric shapes. Dashed lines represent the two wavelengths used in the *Z*-scan experiments. (b) Values of absorbance for different incubation times measured at 532 nm (squares) and 979 nm (circles). Lines indicate values for pure water (continuous, 979 nm; dashed, 532 nm), KBr buffer (lines with open geometric shapes), and $CuSO_4$ buffer (lines with filled geometric shapes).

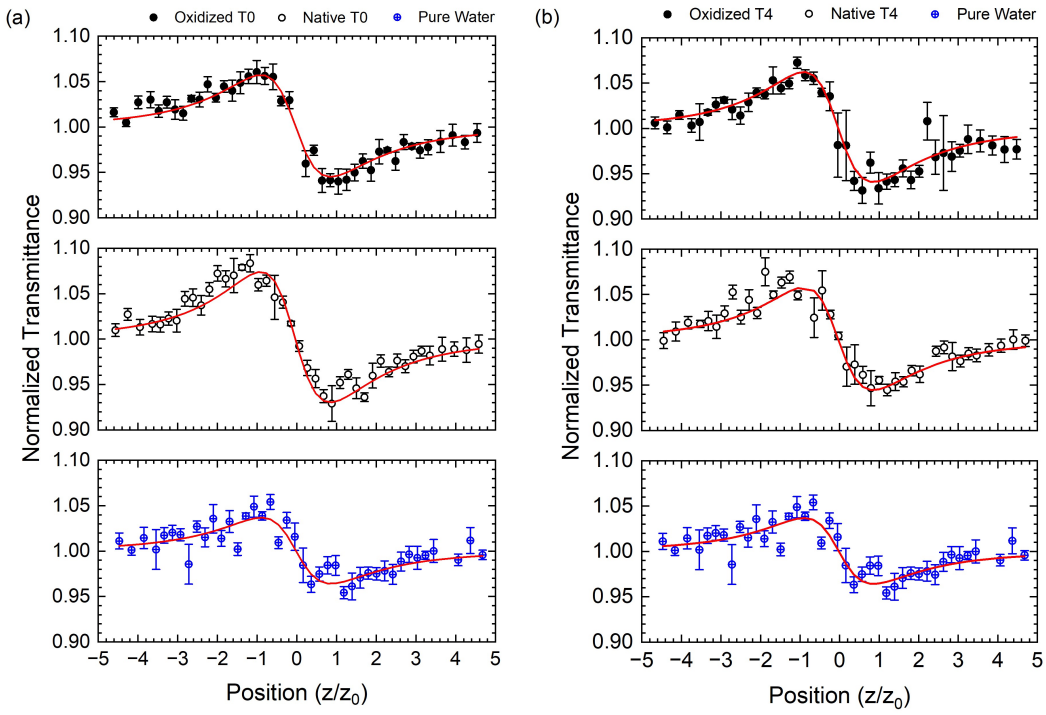

Fig. 2. Z-scan measurements at 979 nm for fresh (open circles) and 6 h incubation (black circles) lipoprotein and pure water (crossed circles) with (a) 5 min incubation samples and (b) 6 h incubation samples. Lines are curves fitted to the experimental data [Eq. (5)]. Exposure time 30 ms; power on the sample 95 mW.

were performed with the beam power of 95 mW, and light-exposition time $t = 30$ ms per cycle. Equation (5) was used to fit the experimental data. Self-defocusing behavior, due to thermal-lens formation, was larger in lipoprotein samples than in pure water, even with the optical absorption of water being bigger than that of the lipoprotein samples. Here, a behavior like that observed in amphiphilic systems, where the thermal response depends on the structure of the amphiphilic aggregates, could take place [53].

Once the ZS curves for all samples are obtained, the behavior of the samples can be investigated in terms of magnitude of the thermal effect and the time needed for the effect to take place. Figure 3 shows the amplitude of the thermal-lens effect (θ) as a function of the exposure time (t), during an interval of 30 ms of exposure to light (in steps of 5 ms). Equation (5) was used to obtain the values of θ.

Observing Fig. 3(a) the fitted phase distortion (θ) values for samples containing LDL are larger than those of pure water for exposures above 10 ms. As seen in Fig. 1(b) the absorbance of pure water is larger than that of samples containing LDL, and this could lead to imagining that the response of pure water should be larger than that of samples with LDL. However, in systems that have structured particles in a solvent, such as LDL or micellar systems, the thermal response arises, besides the temperature profile in the sample, from a collective behavior of the sample components, which amplifies the magnitude [53]. On the other hand, when observing Fig. 3(b), it is possible to compare the response of pure water with the buffers (aqueous media with no structured component) used in the preparation

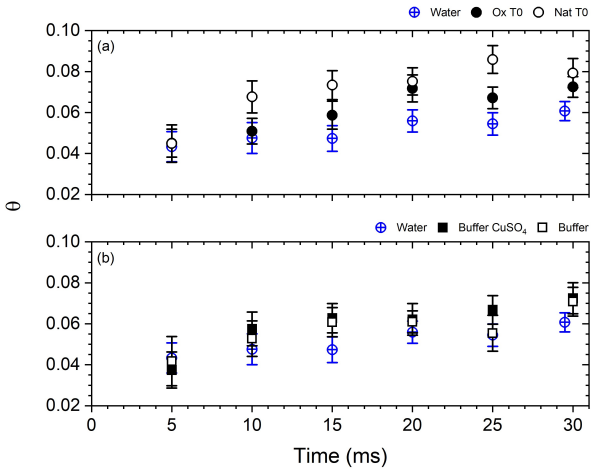

Fig. 3. Amplitude of the thermal-lens effect as a function of the exposure time, during an interval of 30 ms of exposure to light, in the Z-scan experiments: (a) lipoprotein samples; (b) buffers. Crossed circles in both graphs represent water.

of LDL samples (native and oxidized), and it is possible to notice that the phase distortion (θ) values are similar as well as the absorbance values of the media as seen in Fig. 1(b).

The behavior observed in Fig. 3 is similar for samples that undergo incubation. Since the data in Fig. 3 shows a saturation behavior, we propose a simple description of them as in Eq. (6):

$$\theta\,(t) = \theta_{\text{sat}}\left(1 - e^{-\frac{t}{t_{c0}}}\right). \tag{6}$$

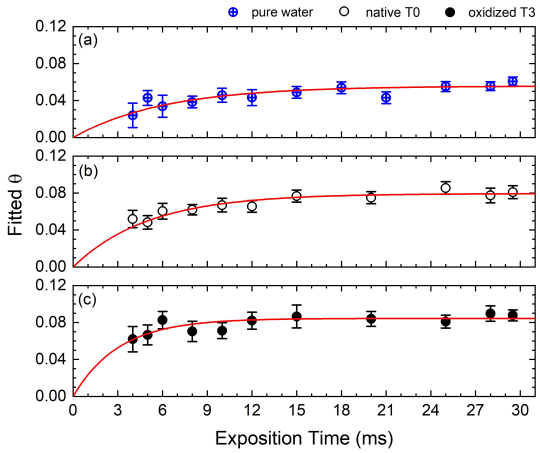

Fig. 4. Time evolution of θ obtained from Z-scan results as a function of the exposure time, during an interval of 30 ms of exposure to light, for (a) water, (b) native, and (c) 5 h oxidized samples and respective fits (solid lines).

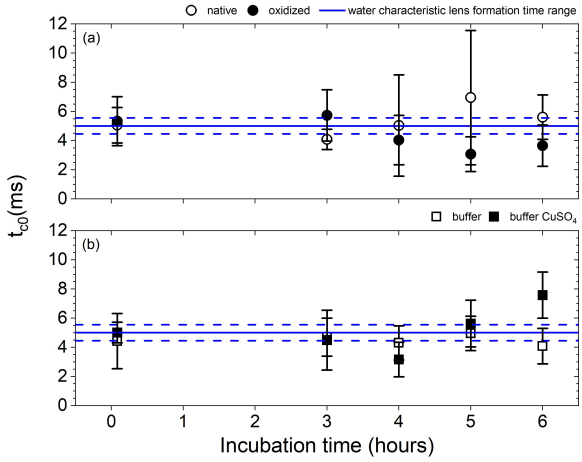

Fig. 5. Characteristic thermal-lens formation time as a function of the incubation time of (a) lipoprotein samples (circles) and (b) buffers (squares) for different incubation times compared to the expected thermal-lens formation time for water (range represented by dashed lines).

This equation gives a quantitative description of the thermal-lens formation, where t_{c0} and θ_{sat} represent the characteristic time of the lens formation and the saturation value of θ. In this way, Eq. (6) allows to fit the θ values obtained from ZS curves at different exposure times. In this simple model, when $t = t_{c0}$, the effect reaches 63% of its saturation value, while for $t = 2t_{c0}$, the effect reaches 86% and for $t = 3t_{c0}$, 95%. The characteristic time of thermal-lens formation is defined elsewhere [4] and is given by Eq. (1). Since the results were obtained with two different experimental setups (of different wavelengths), with different beam waists, according to the t_c definition, it will lead to different thermal-lens formation times for each setup. The characteristic values for the formation of a thermal lens in aqueous samples (using the thermal diffusivity of water, at 37°C, in the calculation: 1.51×10^{-7} m^{2}s^{-1} [54]) for the two experimental setups used are: 5.0 ± 0.5 ms for the IR light and 1.34 ± 0.07 ms for the visible light.

Figure 4 presents values of θ as a function of the exposure time, during an interval of 30 ms of exposure to light, for water, native LDL T0 (5 min incubation), and oxidized LDL T3 (5 h incubation) samples. In the same graph there are fitted curves [Eq. (6)] for the saturable effect, with good agreement in all cases.

The analysis of these response curves indicates that, in terms of the observed effect time evolution, the fitted θ saturation values are similar for LDL samples (oxidized: 0.084 ± 0.005 and native: 0.079 ± 0.005) and higher than pure water (0.056 ± 0.005). From the same fittings it was determined that water needed 14 ± 6 ms for reaching 90% of the saturation θ value ($t \approx 2.3t_{c0}$), a time similar to that observed for the LDL native sample 12 ± 3 ms, but longer than that observed for the oxidized LDL sample 7 ± 3 ms. For comparison purposes, the thermal-lens formation time value determined for water was $t_{c0} = 6.1 \pm 2.7$ ms, which is compatible with the expected [calculated from Eq. (1) for $w = w_0 = 55$ µm and $D = 1.51 \times 10^{-7}$ m^{2}s^{-1} [54], for 37°C] value (5.0 ± 0.5 ms).

Figure 5 shows the characteristic times of thermal-lens formation, t_{c0}, for all lipoprotein samples [Fig. 5(a)] and buffers [Fig. 5(b)]. In both figures there is a range of dashed lines with a line in the middle indicating the calculated time interval of the characteristic response for water thermal-lens formation (dashed lines indicate interval of one standard deviation), for comparison purposes.

As observed in Fig. 5, the characteristic thermal-lens formation times, t_{c0}, present similar values, since the samples are predominantly composed of water. On the other hand, these values are, in general, lower than those experimentally determined for water (6.1 ± 2.7 ms). The buffers, except for the sample with 6 h incubation time, consistently present values that are very close to each other and compatible with the expected value for the water. The lipoprotein samples present a greater dispersion of t_{c0} values, as well as with respect to the expected value for water. The values for native samples do not show a clear trend while the oxidized samples, for incubation values greater than 3 h, present values lower than that of water, with a tendency to decrease, with increasing incubation times. Figure 6 illustrates this discussion.

The t_{c0} values decreasing tendency with the increasing incubation time for oxidized samples is clearly seen in Fig. 6(a), mainly after 3 h of incubation. With the values of t_{c0}, it is possible to calculate [Eq. (3)] the thermal diffusivity of the solution, D, shown in Fig. 6(b).

As these are samples with high water content, the thermal diffusivity values obtained from the thermal-lens formation times are the ones from pure water. Even so, it is possible to notice that the thermal diffusivity values for samples oxidized for more than 3 h increased with respect to the value calculated for the sample without oxidation. This situation is clearly noted in Fig. 6(b). On the other hand, as expressed in Eq. (1), thermal diffusivity is directly proportional to thermal conductivity and inversely proportional to the product of density and heat capacity. One possible explanation for the observed behavior is that the oxidation of the lipoprotein increases the system's capacity to transfer the heat received during the thermal-lens formation process. As

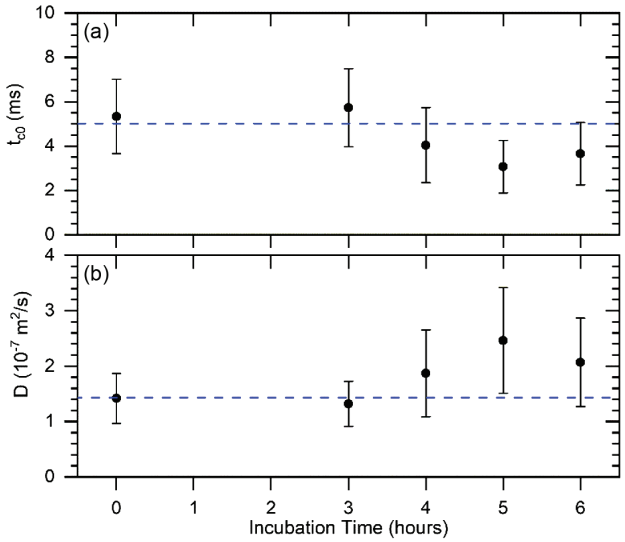

Fig. 6. (a) Thermal-lens formation times, t_{c0}, for oxidized lipoprotein samples at different incubation times. The blue dashed line indicates the calculated t_{c0} value for water. (b) Thermal diffusivity, D, calculated using Eq. (1) for oxidized samples. The blue dashed line indicates the D value for water at 37°C [54].

reported elsewhere, LDL structure changes due to *in vitro* oxidation with $CuSO_4$ [55,56]. The size polydispersity of oxidized LDL (after 18 h incubation) increased, and this effect may be associated with changes in the symmetry of the particle [36]. Moreover, oxidation products, as phospholipids hydroperoxides and cholesterol ester hydroperoxides, are formed in the process. These molecules are much smaller than the LDL particle and may improve the heat transfer across the sample once lipid composition can affect photothermal response [57].

In terms of phase-distortion magnitude, θ_{sat}, the values obtained in the fits were numerically smaller for water than for the other samples: buffers and lipoproteins (oxidized or not).

Data are presented in Fig. S3 of Supplement 1, where θ_{sat} values for samples and buffers are similar and are systematically higher than those obtained for pure water. The amplitude of the thermal lens formed in the oxidized samples (θ_{sat}) are, roughly, higher than those of the native samples, just left at rest in the laboratory. Table 1 presents results of average values of θ_{sat} for LDL samples and buffers (weighted average) and for water. The average values reported in the table indicate that, in addition to the significant difference in θ_{sat} values between the samples and water, it is still possible to notice a difference between the average θ_{sat} value for the oxidized samples with respect to the other samples (native and buffers). This difference is small, but greater than one standard deviation. This result indicates that the oxidation products, produced during the oxidation of the sample, contribute to the formation of the thermal lens, in the case when the heat flows from the solvent to the solute.

B. *Z*-Scan at 532 nm

ZS measurements with the same samples were performed in the 532 nm setup. There are many reported results for lipoproteins investigated with the ZS technique at this wavelength

Table 1. Results of Average θ_{sat} Values for Lipoproteins, Buffers, and Water Samples

Samples	$<\theta$sat$>$
Water	0.056 ± 0.006
Buffers	0.0716 ± 0.0019
Buffers $CuSO_4$	0.0684 ± 0.0018
Native LDLs	0.0688 ± 0.0021
Oxidized LDLs	0.0747 ± 0.0024

[18,19,36,43–45,58,59]. This allows a comparison between our results and published ones.

In these experiments, 200 μm thick lipoprotein samples were exposed to a beam of 100 mW power for 30 ms with 30 ms of resting time after each exposition (conditions similar to those applied in already published results). Water and buffer samples did not generate a thermal lens under these experimental conditions (ZS curves were flat). For lipoprotein samples, it was possible to obtain ZS curves for all native samples (without oxidation) and for oxidized samples up to an incubation time of 5 h. All the samples show negative nonlinearity behavior, as observed in previous papers [18,19,35,36,44,45,58]. The experimental data for the sample with an incubation time of 6 h, under conditions identical to those of the other samples, did not allow the identification of any thermal-lens formation. ZS curves for native and oxidized initial samples (T0) and for an incubation time of 6 h (T4) can be found in Supplement 1, Fig. S4. The native samples showed θ of similar magnitude, while the oxidized sample showed a clear decrease in magnitude of θ with the incubation time, going from a value like those observed for the native samples (T0 and T4) to an undetectable amplitude value. This behavior was not observed for measurements carried out with the IR setup.

As for the measurements carried out with 979 nm wavelength, the observed response of the thermal effect (θ) showed a saturation behavior. The asymptotic value is achieved at about 15 ms exposure time. Figure 7 shows the fitted [Eq. (6)] θ_{sat} values for all native lipoprotein samples and for the three samples that undergo the oxidation process (T0, T1, and T2). The sample with 5 h of incubation time presented results of very low magnitude and for times shorter than 15 ms it was not possible to obtain reliable fittings of the θ values. Therefore, the θ_{sat} value was obtained from the average of the fitted θ values for times between 28.5 and 30 ms. For sample T4, it was not possible to obtain values for θ due to the low magnitude of the effect.

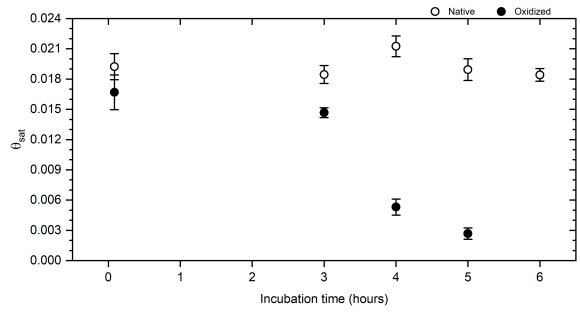

Fig. 7. θ_{sat} values of lipoprotein samples for different incubation times. Incident power of 100 mW, wavelength 532 nm.

Table 2. Amplitude of the Thermal Response and Absorbance Results for Lipoprotein Samples

	532 nm		979 nm	
Sample	θ_{sat}	Absorbance	θ_{sat}	Absorbance
Nat T0	0.0192 ± 0.0013	0.094	0.079 ± 0.005	0.201
Nat T1	0.0184 ± 0.0009	0.089	0.066 ± 0.003	0.204
Nat T2	0.0213 ± 0.0010	0.085	0.058 ± 0.009	0.200
Nat T3	0.0189 ± 0.0011	0.087	0.071 ± 0.015	0.207
Nat T4	0.0184 ± 0.0006	0.087	0.072 ± 0.006	0.205
Ox T0	0.0167 ± 0.0017	0.082	0.068 ± 0.005	0.196
Ox T1	0.0147 ± 0.0005	0.077	0.076 ± 0.006	0.195
Ox T2	0.0053 ± 0.0008	0.058	0.073 ± 0.006	0.196
Ox T3[a]	0.0027 ± 0.0006	0.060	0.084 ± 0.005	0.194
Ox T4	N/A	0.056	0.071 ± 0.005	0.196

[a]θ_{sat} value for the oxidized T3 sample was obtained from the average of θ values for the exposure range [28.5; 30 ms].

It is clear, by observing Fig. 7, that native samples did not show any important variation in the θ_{sat} values as a function of the time, left at rest at a fixed temperature, at least for 6 h. On the other hand, for samples subjected to oxidation, the longer the incubation time, the lower the thermal effect observed. Table 2 presents results where it is possible to directly compare the values obtained from the thermal-lens fits [Eq. (5)], for the native and oxidized samples at different incubation times, for the two wavelengths used in the experimental setups.

5. DISCUSSION

Coming back to the ZS results obtained with 979 mn wavelength, the formation of the thermal lens has a characteristic time t_c, given by Eq. (1), that correlates parameters of the experimental setup–beam waist (w)–and sample physical property–thermal diffusivity (D).

As seen in Fig. 5, the characteristic values of t_{c0} of native and oxidized LDL samples, as well as for buffers, for zero incubation time are about the same. Meanwhile, for the incubation time of 6 h, t_{c0} of the LDL_{ox} sample presents a significant difference with respect to the result for the sample at time zero. Taking the ratio between t_{c0} for LDL_{ox}, T4 ($t_{c0}^{ox}(T4) = 3.7 \pm 1.4$) and LDL_{nat}, T0 ($t_{c0}^{nat}(T0) = 5.1 \pm 1.2$) we have

$$\frac{t_{c0}^{ox}(T4)}{t_{c0}^{nat}(T0)} = 0.7 \pm 0.3.$$

In terms of thermal-lens formation, the fact that the effect occurs more quickly in the oxidized sample than for the native sample means, as Eq. (1) indicates, that the thermal diffusivity of the oxidized (D^{ox}) sample is greater than the thermal diffusivity of the native (D^{nat}) sample, i.e., $t_{c0}^{ox} < t_{c0}^{nat} \Rightarrow D^{ox} > D^{nat}$. Returning to the ratio of t_{c0} values,

$$\frac{t_{c0}^{ox}}{t_{c0}^{nat}} = \frac{D^{nat}}{D^{ox}} = (0.7 \pm 0.3) \rightarrow D^{ox} = (1.4 \pm 0.6)\, D^{nat}.$$

Since the thermal-lens formation time is shorter for oxidized samples, the range of thermal diffusivity values of D^{ox} is [$2.0\,D^{nat}$; $1.0\,D^{nat}$], which is a very wide range. In Fig. 6(b) the diffusivity values for oxidation times greater than 3 h are on the order of 1.5 times the value determined for the initial sample incubation of 5 min (a situation similar to the native sample). There are reported examples of increase in the thermal diffusivity of materials such as the decomposition of $Cu(OH)_2$ into CuO due to ageing [60] or in fluids containing metallic nanoparticles [61]. In the case of LDL samples, a previous result indicates an increase in thermal diffusivity with the sample's oxidation time. The result was obtained for a wavelength of 532 nm and an oxidation time of up to 90 min and, qualitatively, agrees with that obtained [18]. Since water is the main component of the studied samples, C_p is assumed to have very similar values for native and oxidized samples, with negligible variation. According to Eq. (1), variations in thermal diffusivity are related to variations in the ratio of thermal conductivity to sample density. Then, for $D^{ox} > D^{nat}$, it is expected that $\frac{\kappa^{ox}}{\rho^{ox}} > \frac{\kappa^{nat}}{\rho^{nat}}$.

At this point it is worth to mention that the average composition of LDL is: 22% apoB-100 protein, 22% phospholipids, 8% cholesterol, 42% cholesteryl esters, and 6% triglycerides (wt/wt) [62]. A study published with rabbit endothelial cells reported that oxidation caused an increase in the average density of the LDL from 1.036 to 1.070 g/mL [63]. An LDL copper-induced oxidation study quantified the change in the density subclass of LDL components for 20 h of incubation [64]. In those studies, authors concluded that the increase in density due to oxidation is lower than 5%. Assuming $\rho^{ox} \sim 1.02\rho^{nat}$ the relation $\frac{\kappa^{ox}}{\rho^{ox}} > \frac{\kappa^{nat}}{\rho^{nat}}$ can be rewritten as $\frac{\kappa^{ox}}{1.02\rho^{nat}} > \frac{\kappa^{nat}}{\rho^{nat}}$ or $\frac{\kappa^{ox}}{\rho^{nat}} > 1.02\frac{\kappa^{nat}}{\rho^{nat}}$. Finally, $\kappa^{ox} > \kappa^{nat}$.

Coming back to Eq. (4), which describes the phase distortion θ due to the thermal effect, one sees that it depends on both the instrumental parameters (power P, wavelength λ)—kept constant for all measurements—and on the parameters inherent to the samples (optical absorption α, thickness L, thermal conductivity κ, and thermo-optic coefficient $\frac{dn}{dT}$). The sample thickness was kept constant for all measurements. Thus, the ratio between two θ values will be given as a function of α, κ, and $\frac{dn}{dT}$.

By doing some manipulations (presented explicitly in Supplement 1), it is possible to find the relationship of the thermo-optic coefficients for native and oxidized samples:

$$\left|\frac{dn}{dT}\right|^{ox} = (1.6 \pm 0.7)\left|\frac{dn}{dT}\right|^{nat}.$$

These findings indicate an important difference between the thermo-optic coefficients from native to oxidized LDLs. It has already been reported that different structures of fat-water interfaces cause large variations in parameters such as the coefficient of thermal expansion and that, for some lipid systems, an anomalous dependence on temperature may occur [65]. Variations in the coefficient of thermal expansion with temperature cause variations in the density of the medium, modifying its refractive index [66]. Changes in the relative lipid-water composition due to LDL oxidation could lead to changes in the behavior of the thermo-optic coefficient.

It is worth mentioning that the results that allowed the observations presented were only possible because the oxidized samples (as well as the native ones) responded to measurements at 979 nm wavelength. The most oxidized samples did not present a thermal lens detectable response at 532 nm.

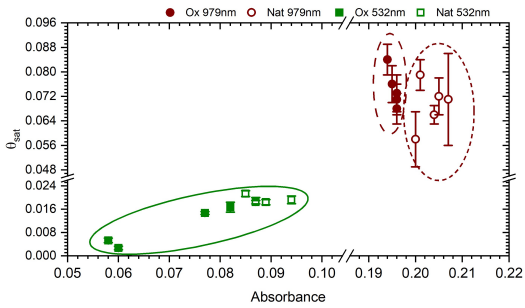

Fig. 8. Behavior of θ_{sat} as a function of the sample absorbance. Squares represent measurements at 532 nm, while circles represent measurements at 979 nm. Native samples, open shapes; oxidized samples, filled shapes. Solid lines: behavior for 532 nm; dashed lines: behavior for 979 nm.

As a final remark, the process of forming the thermal lens heating initially the solvent allowed the obtaining of new information about the LDL particles and their dynamics of oxidation.

A. Comparison between the Results Obtained with Both Wavelengths

Figure 8 shows the behavior of θ_{sat} as a function of the lipoprotein absorbance for the two wavelengths used in ZS experiments (532 nm: squares; 979 nm: circles). It is possible to notice the trend for θ_{sat} as a function of absorbance only for the oxidized sample measured at 532 nm. This behavior at 532 nm was previously observed in studies about the quality of LDL particles in subjects with acute myocardial infarction [45]. The choice of working with "broken axes" arises from the difference in absorbance value ranges for the samples in the two laser wavelengths.

Differently from the results with the visible laser wavelength, those with the IR light do not show a clear dependence with the absorbance. We just guess that the experimental points of the oxidized and the native seem to be grouped. Despite the fact that the values of θ_{sat} of the Ox and Nat spread around 0.072, the absorbance (at 979 nm) of the Nat samples are systematically higher than those from the Ox samples. Moreover, the Ox samples show results that the higher the absorbance, the smaller the θ_{sat}. Since the oxidation process modifies the structure of the LDL particles, with the presence of oxidation products, smaller than the original particles, this new medium with big (LDL particles) and small objects (oxidation products) seems to interfere in the water absorbance, with repercussions on the thermal-lens formation.

An interesting remark of our studies is that, when the thermal-lens formation is mainly due to the solvent, it is possible to investigate properties of the oxidized LDL particles even at higher degrees of oxidation. Therefore, the results obtained by the ZS technique using the 979 nm wavelength for LDL samples oxidized *in vitro* show that the technique has potential for use also with samples oxidized *in vivo*, being a simple, independent, and complementary method to existing techniques for determining oxLDL [37,38].

6. CONCLUSIONS

Time-resolved ZS experiments with water solutions of human lipoproteins (LDLs) by using two laser wavelengths, 532 and 979 nm, are discussed. The processes of formation of the thermal lenses in the samples depend on the laser wavelength. In the experiments at 532 nm, the heating of the sample is due to the light absorption by the carotenoids, present in the LDL, that conduct the heat to the solvent. In the experiments at 979 nm, the solvent is the main absorber of the light that, in the following, conduct the heat to the solute.

Our results showed that the thermal lenses formed in the experiments at 979 nm allowed the obtention of physical parameters of the LDL, regardless of the oxidation degree of the samples. It is worth to stress that the experiments at 532 nm allow the study of native LDLs and those in the early stages of oxidation. Increasing the oxidation degree leads to very small thermal response of the sample (i.e., decreases the peak-to-valley curve), increasing the experimental errors.

The values of θ of oxidized samples, determined using the IR setup, are bigger than those obtained for native LDL samples. The characteristic lens-formation time for the oxidized samples showed an interesting behavior, with a tendency to decrease with increasing oxidation time. This behavior may be due to the presence of oxidation products in the sample, which improves the heat transfer across the sample.

Moreover, employing the 979 nm laser setup it was possible to estimate relations between the thermal conductivities and thermo-optic coefficients of the native and samples subjected to a high degree of oxidation, not possible with the usual 532 nm laser setup.

Funding. Fundação de Amparo à Pesquisa do Estado de São Paulo (2014/50983-3, 2016/24531-3); Instituto Nacional de Ciência e Tecnologia de Fluidos Complexos; Coordenação de Aperfeiçoamento de Pessoal de Nível Superior; Conselho Nacional de Desenvolvimento Científico e Tecnológico (465259/2014-6).

Acknowledgment. The authors would like to thank D. Reis, M.Sc., for his support in absorbance measurements and data processing related to these measurements. The authors also thank "COLSAN - Associação Beneficiente de Coleta de Sangue, São Paulo, Brazil" for providing the biological material used for obtaining the LDL samples.

Disclosures. The authors declare no conflicts of interest.

Data availability. Data underlying the results presented in this paper are not publicly available at this time but may be obtained from the authors upon reasonable request.

Supplemental document. See Supplement 1 for supporting content.

REFERENCES

1. M. Sheik-Bahae, A. A. Said, T. H. Wei, *et al.*, "Sensitive measurements of optical nonlinearities using a single beam," IEEE J. Quantum Electron. **26**, 760–769 (1990).
2. R. M. Moysés, E. C. Barbano, and L. Misoguti, "Discrimination of thermal, molecular orientation, and pure electronic refractive nonlinearities using the polarization-resolved Z-scan technique," J. Opt. Soc. Am. B **40**, C60–C66 (2023).
3. L. C. Oliveira and S. C. Zílio, "Single-beam time resolved z-scan measurements of slow absorbers," Appl. Phys. Lett. **65**, 2121–2123 (1994).
4. C. A. Carter and J. M. Harris, "Comparison of models describing the thermal lens effect," Appl. Opt. **23**, 476–481 (1984).

5. F. L. S. Cuppo, A. M. Figueiredo Neto, S. L. Gómez, *et al.*, "Thermal-lens model compared with the Sheik-Bahae formalism in interpreting Z-scan experiments on lyotropic liquid crystals," J. Opt. Soc. Am. B **19**, 1342–1348 (2002).
6. S. Alves, A. Bourdon, and A. M. Figueiredo Neto, "Generalization of the thermal lens model formalism to account for thermodiffusion in a single-beam Z-scan experiment: determination of the Soret coefficient," J. Opt. Soc. Am. B **20**, 713–718 (2003).
7. S. L. Gómez, F. L. S. Cuppo, A. M. Figueiredo Neto, *et al.*, "Z-scan measurement of the nonlinear refractive indices of micellar lyotropic liquid crystals with and without the ferrofluid doping," Phys. Rev. E **59**, 3059–3063 (1999).
8. S. L. Gómez, R. F. Turchiello, M. C. Jurado, *et al.*, "Thermal-lens effect of low-density lipoprotein lyotropic-like aggregates investigated by using the Z-scan technique," Liq. Cryst. Today **15**(1), 1–3 (2006).
9. S. Alves, G. Demouchy, A. Bee, *et al.*, "Investigation of the sign of the Soret coefficient in different ionic and surfacted magnetic colloids using forced Rayleigh scattering and single-beam Z-scan techniques," Philos. Mag. **83**(17–18), 2059–2066 (2003).
10. S. Krekic, T. Zakar, Z. Gombos, *et al.*, "Nonlinear optical investigation of microbial chromoproteins," Front. Plant Sci. **11**, 547818 (2020).
11. A. N. Dhinaa and P. K. Palanisamy, "Z-scan technique for measurement of total cholesterol and triglycerides in blood," J. Innov. Opt. Health Sci. **2**, 295–301 (2009).
12. A. N. Dhinaa, A. Y. Nooraldeen, K. Murali, *et al.*, "Z-Scan technique as a tool for the measurement of blood glucose," Laser Phys. **18**, 1212–1216 (2008).
13. A. Ghader, M. H. Ara, S. Mohajer, *et al.*, "Investigation of nonlinear optical behavior of creatinine for measuring its concentration in blood plasma," Optik **158**, 231–236 (2018).
14. G. Reyes-Soffer, H. N. Ginsberg, L. Berglund, *et al.*, "Lipoprotein(a): a genetically determined, causal, and prevalent risk factor for atherosclerotic cardiovascular disease: a scientific statement from the American Heart Association," Arteriosclerosis Thrombosis Vasc. Biol. **42**, e48–e60 (2022).
15. F. Duarte Lau and R. P. Giugliano, "Lipoprotein(a) and its significance in cardiovascular disease: a review," JAMA Cardiol. **7**, 760–769 (2022).
16. P. W. Siri-Tarino and R. M. Krauss, "The early years of lipoprotein research: from discovery to clinical application," J. Lipid Res. **57**, 1771–1777 (2016).
17. K. R. Feingold, "Lipid and lipoprotein metabolism," Endocrinol. Metab. Clin. North Am. **51**, 437–458 (2022).
18. P. Santos, T. C. Genaro-Mattos, A. M. Monteiro, *et al.*, "Behavior of the thermal diffusivity of native and oxidized human low-density lipoprotein solutions studied by the *Z*-scan technique," J. Biomed. Opt. **17**, 105003 (2012).
19. A. M. Monteiro, M. A. N. Jardini, V. Giampaoli, *et al.*, "Measurement of the nonlinear optical response of low-density lipoprotein solutions from patients with periodontitis before and after periodontal treatment: evaluation of cardiovascular risk markers," J. Biomed. Opt. **17**, 115004 (2012).
20. S. Kedenburg, M. Vieweg, T. Gissibl, *et al.*, "Linear refractive index and absorption measurements of nonlinear optical liquids in the visible and near-infrared spectral region," Opt. Mater. Express **2**, 1588–1611 (2012).
21. G. C. Chen and J. P. Kane, "Contribution of carotenoids to the optical activity of human serum low-density lipoprotein," Biochemistry **13**, 3330–3335 (1974).
22. L. B. Sicchieri, A. M. Monteiro, R. E. Samad, *et al.*, "Study of tryptophan lifetime fluorescence following low-density lipoprotein modification," Appl. Spectrosc. **67**, 379–384 (2013).
23. H. Tapiero, D. M. Townsend, and K. D. Tew, "The role of carotenoids in the prevention of human pathologies," Biomed. Pharmacother. **58**, 100–110 (2004).
24. J. M. Zingg, A. Vlad, and R. Ricciarelli, "Oxidized LDLs as signaling molecules," Antioxidants **10**, 1184 (2021).
25. H. McNulty, R. F. Jacob, and R. Preston Mason, "Biologic activity of carotenoids related to distinct membrane physicochemical interactions," Am. J. Cardiol. **101**, 20D–29D (2008).
26. N. Cardinault, J. Abalain, B. Sairafi, *et al.*, "Lycopene but not lutein nor zeaxanthin decreases in serum and lipoproteins in age-related macular degeneration patients," Clin. Chim. Acta **357**, 34–42 (2005).
27. J. E. Romanchik, D. W. Morel, and E. H. Harrison, "Distributions of carotenoids and α-tocopherol among lipoproteins do not change when human plasma is incubated in vitro," J. Nutr. **125**, 2610–2617 (1995).
28. C. S. Boon, D. J. McClements, J. Weiss, *et al.*, "Factors influencing the chemical stability of carotenoids in foods," Crit. Rev. Food Sci. Nutr. **50**, 515–532 (2010).
29. A. J. Meléndez-Martínez, C. M. Stinco, P. M. Brahm, *et al.*, "Analysis of carotenoids and tocopherols in plant matrices and assessment of their in vitro antioxidant capacity," Methods Mol. Biol. **1153**, 77–97 (2014).
30. E. Ashenafi, M. C. Nyman, J. T. Shelley, *et al.*, "Spectral properties and stability of selected carotenoid and chlorophyll compounds in different solvent systems," Food Chem. Adv. **2**, 100178 (2023).
31. M. Hagos, M. Redi-Abshiro, B. S. Chandravanshi, *et al.*, "Development of analytical methods for determination of β-carotene in pumpkin (cucurbita maxima) flesh, peel, and seed powder samples," Int. J. Anal. Chem. **2022**, 9363692 (2022).
32. P. S. Bernstein and R. Arunkumar, "The emerging roles of the macular pigment carotenoids throughout the lifespan and in prenatal supplementation," J. Lipid Res. **62**, 100038 (2021).
33. J. Udensi, J. Loughman, E. Loskutova, *et al.*, "Raman spectroscopy of carotenoid compounds for clinical applications-a review," Molecules **27**, 9017 (2022).
34. D. J. Lamb and D. S. Leake, "The effect of EDTA on the oxidation of low density lipoprotein," Atherosclerosis **94**, 35–42 (1992).
35. S. L. Gómez, A. M. Monteiro, S. R. Rabbani, *et al.*, "Cu and Fe metallic ions-mediated oxidation of low-density lipoproteins studied by NMR, TEM and Z-scan technique," Chem. Phys. Lipids **163**, 545–551 (2010).
36. C. L. P. Oliveira, P. R. Santos, A. M. Monteiro, *et al.*, "Effect of oxidation on the structure of human low- and high-density lipoproteins," Biophys. J. **106**, 2595–2605 (2014).
37. H. Itabe and M. Ueda, "Measurement of plasma oxidized low-density lipoprotein and its clinical implications," J. Atheroscler. Thromb. **14**, 1–11 (2007).
38. M. T. Macvanin, J. Stanimirovic, and E. R. Isenovic, "Methods for measurements of oxidized LDL, homocysteine and nitric oxide as clinical parameters of oxidative stress and endothelial dysfunction," Curr. Anal. Chem. **18**, 1040–1056 (2022).
39. J. P. Gordon, R. C. C. Leite, R. S. Moore, *et al.*, "Long-transient effects in lasers with inserted liquid samples," J. Appl. Phys. **36**, 3–8 (1965).
40. C. Hu and J. R. Whinnery, "New thermooptical measurement method and a comparison with other methods," Appl. Opt. **12**, 72–79 (1973).
41. J. R. Whinnery, "Laser measurement of optical absorption in liquids," Acc. Chem. Res. **7**, 225–231 (1974).
42. S. J. Sheldon, L. V. Knight, and J. M. Thorne, "Laser-induced thermal lens effect: a new theoretical model," Appl. Opt. **21**, 1663–1669 (1982).
43. J. Shen, R. D. Lowe, and R. D. Snook, "A model for cw laser induced mode-mismatched dual-beam thermal lens spectrometry," Chem. Phys. **165**, 385–396 (1992).
44. M. C. P. de Freitas, A. M. Figueiredo Neto, and N. R. Damasceno, "Nonlinear optical responses of oxidized low-density lipoprotein: cutoff point for Z-scan peak-valley distance," Photodiagn. Photodyn. Ther. **30**, 101689 (2020).
45. Z. Lotfollahi, A. P. Q. Mello, F. A. H. Fonseca, *et al.*, "Changes in lipoproteins associated with lipid-lowering and antiplatelet strategies in patients with acute myocardial infarction," PLoS One **17**, e0273292 (2022).
46. A. Yariv, *Quantum Electronics*, 3rd ed. (Wiley, 1987).
47. D. W. Swinkels, H. L. M. Hak-Lemmers, and P. N. M. Demacker, "Single spin density gradient ultracentrifugation method for the detection and isolation of light and heavy low density lipoprotein subfractions," J. Lipid Res. **28**, 1233–1239 (1987).
48. B. A. Griffin, M. J. Caslake, B. Yip, *et al.*, "Rapid isolation of low density lipoprotein (LDL) subfractions from plasma by density gradient ultracentrifugation," Atherosclerosis **83**, 59–67 (1990).

49. H. Takano, M. Kondo, N. Usui, *et al.*, "Involvement of CarA/LitR and CRP/FNR family transcriptional regulators in light-induced carotenoid production in Thermus thermophilus," J. Bacteriol. **193**, 2451–2459 (2011).
50. D. Tátraaljai, L. Major, E. Földes, *et al.*, "Study of the effect of natural antioxidants in polyethylene: performance of β-carotene," Polym. Degrad. Stab. **102**, 33–40 (2014).
51. J. M. Khosrofian and B. A. Garetz, "Measurement of a Gaussian laser beam diameter through the direct inversion of knife-edge data," Appl. Opt. **22**, 3406–3410 (1983).
52. S. L. Gómez, R. F. Turchiello, M. C. Jurado, *et al.*, "Characterization of native and oxidized human low-density lipoproteins by the Z-scan technique," Chem. Phys. Lipids **132**, 185–195 (2004).
53. F. L. S. Cuppo and A. M. Figueiredo Neto, "Thermal and nonlinear optical properties of potassium laurate/water solutions at amphiphilic concentrations around the critical micellar concentration: a laser Gaussian single beam experiment in millisecond timescales," Langmuir **18**, 9647–9653 (2002).
54. J. W. Valvano, J. R. Cochran, and K. R. Diller, "Thermal conductivity and diffusivity of biomaterials measured with self-heated thermistors," Int. J. Thermophys. **6**, 301–311 (1985).
55. R. Chehin, D. Rengel, J. C. G. Milicua, *et al.*, "Early stages of LDL oxidation: apolipoprotein B structural changes monitored by infrared spectroscopy," J. Lipid Res. **42**, 778–782 (2001).
56. J. Gallego-Nicasio, G. López-Rodríguez, R. Martínez, *et al.*, "Structural changes of low density lipoproteins with Cu2+ and glucose induced oxidation," Biopolymers **72**, 514–520 (2003).
57. M. Salimi, M. Villiger, and N. Tabatabaei, "Effects of lipid composition on photothermal optical coherence tomography signals," J. Biomed. Opt. **25**, 120501 (2020).
58. S. Alves and A. M. Figueiredo Neto, "Advances in the non-linear optical investigation of lyotropic-like low-density human lipoproteins in the native and oxidised states," Liq. Cryst. **41**, 465–470 (2014).
59. Z. Lotfollahi, A. P. Q. Mello, E. S. Costa, *et al.*, "Green-banana biomass consumption by diabetic patients improves plasma low-density lipoprotein particle functionality," Sci. Rep. **10**, 12269 (2020).
60. R. Sebastian, M. S. Swapna, V. Raj, *et al.*, "Laser-induced thermal lens study of the role of morphology and hydroxyl group in the evolution of thermal diffusivity of copper oxide," Chin. Phys. B **30**, 067801 (2021).
61. J. F. Sánchez Ramírez, J. L. Jiménez Pérez, R. Carbajal Valdez, *et al.*, "Thermal diffusivity measurements in fluids containing metallic nanoparticles using transient thermal lens," Int. J. Thermophys. **27**, 1181–1188 (2006).
62. E. V. Orlova, M. B. Sherman, W. Chiu, *et al.*, "Three-dimensional structure of low density lipoproteins by electron cryomicroscopy," Proc. Natl. Acad. Sci. USA **96**, 8420–8425 (1999).
63. T. Henriksen, E. M. Mahoney, and D. Steinberg, "Enhanced macrophage degradation of biologically modified low density lipoproten," Arteriosclerosis **3**, 149–159 (1983).
64. T. Kidoa, K. Kondob, H. Itakurac, *et al.*, "Sequential change in physicochemical properties of LDL during oxidative modification," Chem. Phys. Lipids **193**, 52–62 (2015).
65. A. Raudino, F. Zuccarello, C. La Rosa, *et al.*, "Thermal expansion and compressibility coefficients of phospholipid vesicles: experimental determination and theoretical modeling," J. Phys. Chem. **94**, 4217–4223 (1990).
66. W. J. Tropf and M. E. Thomas, "Infrared refractive index and thermo-optic coefficient measurement at APL," Johns Hopkins APL Tech. Dig. **19**, 293–298 (1998).